

Hadronic B_u and B_d decays

W. T. Ford
 University of Colorado, Boulder, CO 80309-0390

I present latest measurements from the B factories of branching fractions for B meson decays to hadronic two- and three-body final states. These include the rate of doubly Cabibbo-suppressed charge states of charmed mesons in two-body decays, charmed baryons and other structure seen in baryonic B decays, and charmless mesonic two-body decays in comparison with estimates from theory.

1. Introduction

The PEP-II and KEKB B factories have very recently produced a number of new measurements or limits for B decay modes to hadronic final states. These include some $b \rightarrow c$ modes bearing on the interpretation of experiments aiming to measure the CKM angle γ (ϕ_3), charmless baryonic three-body final states with their two-body substructure, and a number of charmless branching fractions and charge asymmetries. The latter include modes with η , η' , and other pseudoscalar (P - P) combinations, as well as those with vector (V) or axial-vector (A) mesons. I present these experimental results and provide an indication of how the theoretical predictions stack up against all of the currently available measurements. A number of interesting measurements are not included in this review simply because of the limited time.

The experimental identification of B mesons from the decay of the $\Upsilon(4S)$ makes use of the kinematic variables energy-substituted mass

$$m_{\text{ES}} \text{ (or } m_{bc}) \equiv \sqrt{\left(\frac{1}{2}s + \mathbf{p}_0 \cdot \mathbf{p}_B\right)^2 / E_0^2 - \mathbf{p}_B^2} \quad (1)$$

and the energy difference

$$\Delta E \equiv E_B^* - \frac{1}{2}\sqrt{s}, \quad (2)$$

where s is the squared center-of-mass energy, (E_0, \mathbf{p}_0) and (E_B, \mathbf{p}_B) are the laboratory four-momenta of the $\Upsilon(4S)$ and the B candidate, respectively, and the asterisk denotes the $\Upsilon(4S)$ rest frame.

2. Decays Related to $\sin 2\beta + \gamma$

The experiments that determine angles of the unitarity triangle of the CKM matrix are discussed in other talks at this conference, but I mention here a couple of supporting measurements. One can study the decays of B^0 to charged D or D^* mesons in combination with a charged pion or ρ meson [1]. The weak phases are measurable in principle because these final

states can be reached from both B^0 and \bar{B}^0 initial states. We must distinguish however between $b \rightarrow c$ leading to $D^{(*)+}$ and the mixing oscillation $b \rightarrow \bar{b}$ followed by the doubly Cabibbo-suppressed (DCSD) $\bar{b} \rightarrow \bar{u}W^+$, $W^+ \rightarrow D^{(*)+}$. The box diagram responsible for mixing brings in (in the Wolfenstein phase convention) a phase 2β , while the DCSD amplitude brings in γ . The coefficient S^\pm of the $\sin \Delta m_d \Delta t$ term in the time-dependent rate for decays to (\pm) -charged $D^{(*)}$ is given by

$$S^\pm = \frac{2(-1)^L r \sin(2\beta + \gamma \pm \delta)}{1 + r^2}. \quad (3)$$

Here $r \ll 1$ is the ratio of the DCSD amplitude to the Cabibbo-allowed one, δ is the strong phase, and L is the orbital angular momentum between the daughter mesons. The sensitivity is determined by the value of r .

One way to measure r is from the branching fraction ratio

$$r(D^*\pi) = \sqrt{\frac{\tau_{B^0} 2\mathcal{B}(B^+ \rightarrow D^{*+}\pi^0)}{\tau_{B^+} \mathcal{B}(B^0 \rightarrow D^{*-}\pi^+)}} \quad (4)$$

where we assume isospin symmetry [2]. This measurement has been performed by Belle [3] with an exposure of 657 million B pairs. Distributions of

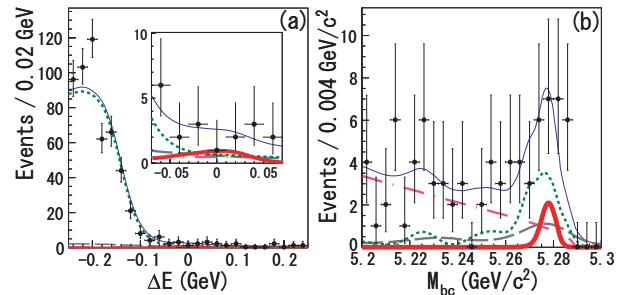


Figure 1: Distributions in (a) ΔE and (b) energy-substituted B mass of candidates for $B^+ \rightarrow D^{*+}\pi^0$ in the Belle data. The points with error bars represent the data, while the curves represent the various components from the fit: signal (thick solid), continuum (dash-dotted), $\bar{B}^0 \rightarrow D^{*+}\rho^-$ decay (dotted), other B decays (dashed), and the sum of all components (thin solid).

the B -decay kinematic variables are shown in Fig. 1. No clear signal is seen, and the result quoted is $\mathcal{B}(B^+ \rightarrow D^{*+}\pi^0) < 3.6 \times 10^{-6}$, leading to the limit

$$r(D^*\pi) < 0.051 \quad (90\% \text{ CL}).$$

A second approach to the determination of r is to employ $SU(3)$ to relate branching fractions of B^0 decays to $D_s^{(*)}$ and a pion or ρ meson:

$$r(D^{(*)}\pi) = \tan\theta_c \frac{f_{D^{(*)}}}{f_{D_s^{(*)}}} \sqrt{\frac{\mathcal{B}(B^0 \rightarrow D_s^{(*)+}\pi^-)}{\mathcal{B}(B^0 \rightarrow D^{(*)-}\pi^+)}}. \quad (5)$$

The *BABAR* collaboration have measured a number of these and related decays [4]. The signals for two representative modes can be seen in Fig. 2. From the

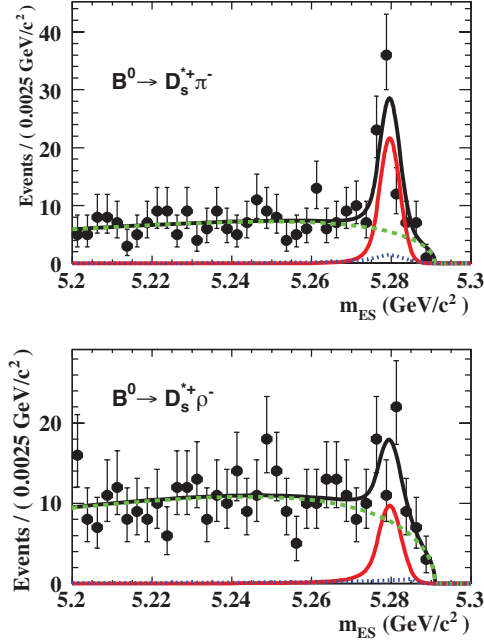


Figure 2: Energy-substituted-mass distributions for $B^0 \rightarrow D_s^{*+}\pi^-$ and $B^0 \rightarrow D_s^{*+}\rho^-$ for the *BABAR* data set of 381 million $B\bar{B}$ pairs; this is first evidence, at 3.9 sigma, for the latter decay mode. The curves represent the fit function (solid), signal (shaded), peaking background (dotted), and continuum background (dashed).

branching fraction measurements and the ratios of decay constants from lattice gauge calculations, the following values are inferred for the various DCSD fractions r :

$$\begin{aligned} r(D\pi) &= [1.75 \pm 0.14 \pm 0.09 \pm 0.10] \times 10^{-2} \\ r(D^*\pi) &= [1.81_{-0.14}^{+0.17} \pm 0.12 \pm 0.10] \times 10^{-2} \\ r(D\rho) &= [0.71_{-0.26}^{+0.29} \pm 0.11 \pm 0.04] \times 10^{-2} \\ r(D^*\rho) &= [1.50_{-0.21}^{+0.22} \pm 0.16 \pm 0.08] \times 10^{-2}; \end{aligned}$$

the first error quoted is statistical, the second experimental systematic, and the third theoretical. Belle's limit above is consistent with these results.

The small value of r resulting from all of these measurements unfortunately limits the sensitivity of the measurements of $2\beta + \gamma$.

3. Three-body Baryonic Modes

3.1. $B \rightarrow p\bar{p}K^{(*)}$

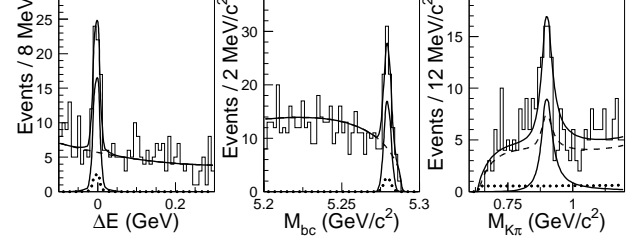


Figure 3: Distributions for $p\bar{p}K^{*0}$ candidates in ΔE , energy-constrained mass, and $K\pi$ invariant mass from the Belle data, 535 million $B\bar{B}$ pairs. The curves show the full fit function (upper solid) together with the components representing signal (lower solid), continuum background (dashed), and non-resonant $K\pi$ background (dotted).

The Belle collaboration have made a thorough investigation over the years of B decays to $p\bar{p}K^{(*)}$, of which the most recent edition reports the observation of $B^0 \rightarrow p\bar{p}K^{*0}$ (Fig. 3) [5]. For each of these final states a substantial threshold enhancement is seen in the $p\bar{p}$ invariant mass spectrum. For those low- $p\bar{p}$ -mass events the K^* helicity distributions show an interesting structure, as indicated in Fig. 4. The fraction of longitudinal polarization is quite different in the two K^* charge states, consistent with 100% for $B^0 \rightarrow p\bar{p}K^{*0}$.

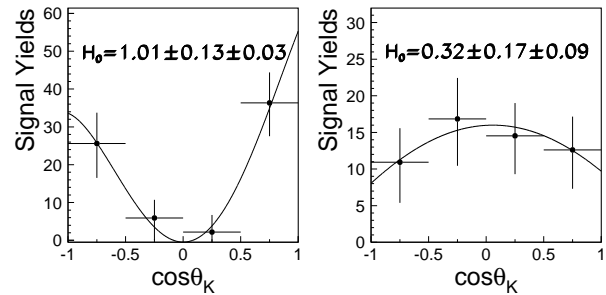


Figure 4: Distributions in the K^* -helicity angle for $p\bar{p}K^{*0}$ (left) and $p\bar{p}K^{*+}$ (right), for events with $m(p\bar{p}) < 2.8$ GeV. Values of the helicity-zero fraction H_0 are given on the plots.

3.2. Σ_c States in B decay

The *BABAR* Collaboration have performed an analysis of the decay $B^- \rightarrow \Lambda_c^+ \bar{p} \pi^-$ of which I present

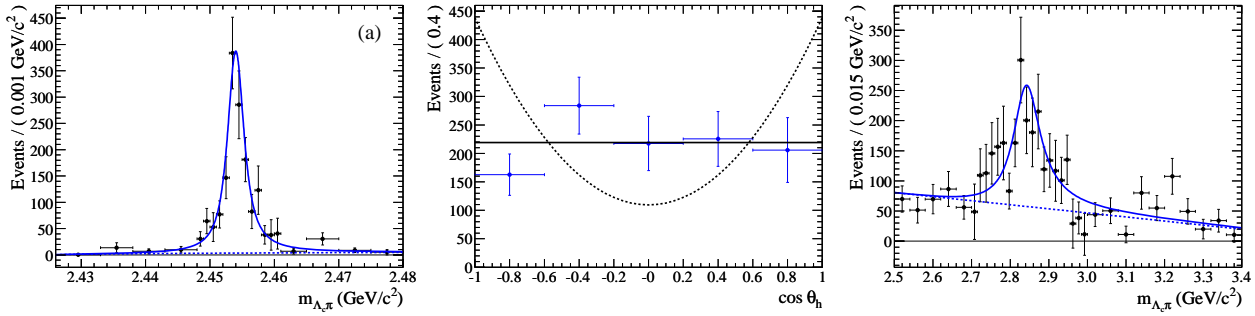


Figure 5: *BABAR* study of $B^- \rightarrow \Lambda_c^+ \bar{p} \pi^-$, based on 383 million $B\bar{B}$. The plots show distributions in $m(\Lambda_c^+ \pi^-)$ for the $\Sigma_c(2455)$ region (left), and the $\Sigma_c(2800)$ region (right). The solid curve shows the fit function, and the dotted curve the background component. The middle plot gives the distribution in helicity cosine for the events in the $\Sigma_c(2455)$ peak, with predictions for spin- $\frac{1}{2}$ (solid) and $\frac{3}{2}$ (dotted).

an update here [6]. The Dalitz plot shows a threshold enhancement in the $\Lambda_c^+ \bar{p}$ invariant mass spectrum, reminiscent of that seen in $p\bar{p}K^{(*)}$. In addition it shows clear peaks in $m(\Lambda_c^+ \pi^-)$ corresponding to the known resonance at 2455 MeV and a second state at 2800 MeV. These projections are shown in Fig. 5. The helicity-angular distribution allows a determination for the first time of the spin of the $\Sigma_c(2455)$; $J = \frac{1}{2}$ is strongly favored over $J = \frac{3}{2}$, with the assumption that the Λ_c itself is spin- $\frac{1}{2}$.

There is no evidence in the *BABAR* data of the $\Sigma_c(2520)$. The second resonance that is seen has a mass of $2846 \pm 8 \pm 10$ MeV and width 86^{+33}_{-22} MeV (right plot in Fig. 5). One may ask if this is the same as the isotriplet $\Sigma_c(2800)$ produced in continuum e^+e^- annihilation as seen previously by Belle [7]. The data for Belle’s state suggest a spin assignment $J = \frac{3}{2}$. Since the resonance masses determined by *BABAR* and Belle differ by three sigma, they may be distinct resonances. A conjecture offered by the *BABAR* authors is that $J = \frac{3}{2}$ states are suppressed in B decays, accounting for the absence of $\Sigma_c(2520)$, and that they are seeing a new $\Sigma_c(2850)$ with $J = \frac{1}{2}$, rather than the $\Sigma_c(2800)$.

4. Charmless Mesonic Decays

I report next on the latest progress in the study of B decays to meson pairs, an area of vigorous activity that aims to map out the many channels experimentally and to understand them theoretically, or at least to characterize them phenomenologically. The presence of non-perturbative hadronic effects complicates the picture, but the large energy release in these heavy to light decays provides the possibility to control those uncertainties. The number of charmless mesonic decays that have been observed experimentally and listed in the Heavy Flavor Averaging Group compilations [8] is approaching a hundred, with limits

established for many more.

4.1. Theoretical Estimates of Branching Fractions and Charge Asymmetries

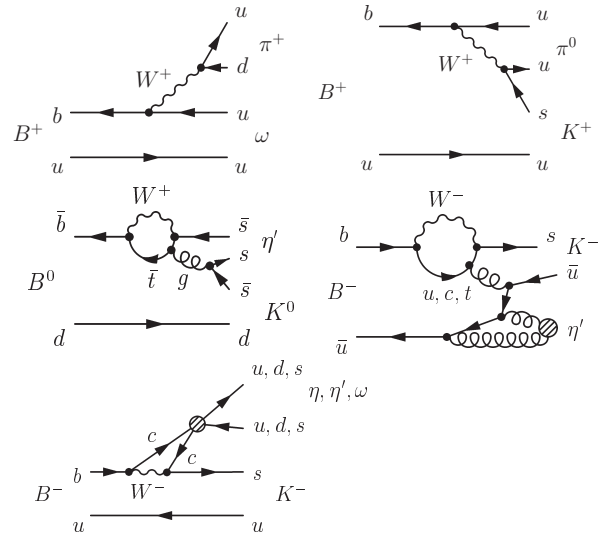


Figure 6: Representative Feynman diagrams for charmless B meson decays: (upper left) external tree ($\Delta S = 0$, T); (upper right) color-suppressed tree ($|\Delta S| = 1$, C'); (middle left) gluonic penguin (P'); (middle right) flavor singlet penguin (S'); (bottom) “charming penguin”.

At the parton level these processes are mediated by amplitudes represented by diagrams like those shown in Fig. 6. One phenomenological approach to the estimation of decay rates and charge asymmetries identifies a reduced matrix element with each of the parton topologies and relates their contributions to the various decay modes via flavor- $SU(3)$ symmetry [9, 10]. Seven independent reduced diagrams and the CKM angle γ are fit to all of the available data within each

of the final-state particle classes P - P , P - V_s , and P_s - V , where P is a pseudoscalar meson, V is vector meson, and the subscript indicates the meson containing the spectator quark. The seven topologies are the first four named in the Fig. 6 caption, plus weak annihilation (a), W -boson exchange (e) and penguin annihilation (pa). This picture is found to be quite compatible with the data as indicated by the fit chisquares, and Figures 8 and 9 below.

The direct calculation of decay rates and charge asymmetries begins with the effective Hamiltonian written as an operator product expansion (OPE) [11]. For a $b \rightarrow s$ transition:

$$\mathcal{H}_{\text{eff}} = \frac{G_F}{\sqrt{2}} \sum_{p=u,c} V_{ps}^* V_{pb} \left(C_1 Q_1^p + C_2 Q_2^p + \sum_{i=3}^{10} C_i Q_i + C_{7\gamma} Q_{7\gamma} + C_{8g} Q_{8g} \right) + \text{h.c.} \quad (6)$$

The operators correspond to terms in the full theory at parton level as

- $Q_{1,2}^p$: current-current operators from W exchange
- $Q_{3\dots 6}$: local 4-quark QCD penguin operators
- $Q_{7\dots 10}$: local 4-quark electroweak γ, g, Z penguin, and W box operators
- $Q_{7\gamma}$: electromagnetic dipole operator
- Q_{8g} : chromomagnetic dipole operator,

while $C_i, C_{7\gamma}, C_{8g}$ are the Wilson coefficient functions. The factorization of each term facilitates the calculation by separating factors calculable, to next-to-leading order (NLO) in the strong coupling constant α_s , from QCD and the renormalization group. This separation is however scale- and scheme-dependent, requiring that the matrix elements be calculated to matching order in the same scheme and scale. The matrix elements include the problematic long-distance effects.

The factorization ansatz for dealing with the hadronic matrix elements employs the concept of ‘‘color transparency’’: because of the large Q -value in a heavy quark decay the daughter mesons fly from the region of their formation so quickly that their soft hadronic interactions are suppressed (by a factor of order Λ_{QCD}/m_b). The matrix element becomes a product of a form factor, representing the transition of the B to one meson, and a decay constant, representing the creation from vacuum of the other daughter meson. Some of the earlier applications [12] treat quark masses and the effective number of colors as free parameters in fits to data.

The naive factorization method has been improved upon (‘‘QCD factorization’’, QCDF [13, 14]) with the

inclusion of terms that account for interactions with the spectator quark. The hard-scattering kernels are calculated in the heavy quark limit at NLO, while non-perturbative effects are absorbed into form factors and light-cone parton distribution functions that are taken as inputs to the calculation.

Some of the calculations have been improved with the use of soft-collinear effective theory (SCET) [15], which provides techniques for dealing with the very different energy scales between the leading quarks and soft glue.

An alternative improvement on naive factorization is provided by the ‘‘perturbative QCD’’ framework (pQCD) [16–18]. In this approach the treatment of the parton transverse momentum serves to control endpoint singularities in the parton distribution functions, allowing the calculation of heavy-to-light form factors. In these calculations penguin annihilation terms are found to give substantial, imaginary contributions that correspond to direct CP violation.

The ‘‘charming penguins’’ approach [19] incorporates factorization-violating terms of $\mathcal{O}(\Lambda_{\text{QCD}}/m_b)$, especially the penguin terms with charm quarks in the loop. The small number of unknown complex amplitudes can be obtained from fits to data.

4.2. $\Delta S = 1$ Decays

The importance of penguin amplitudes is demonstrated by the prominence of modes with (an odd number of) kaons among those with the largest branching fractions. The first of these to be seen were $B^0 \rightarrow K^+\pi^-$ and, with a surprisingly large strength, $B \rightarrow \eta'K$. The need to explain the latter motivated some of the theoretical ideas alluded to above, including the flavor-singlet (η' strongly coupled to glue) and charming penguin (η' strongly coupled to $c\bar{c}$) pictures. A large value of the branching ratio $\Gamma(B \rightarrow \eta'K)/\Gamma(B \rightarrow \eta K)$ is consistent with interference between the penguin amplitudes in which the created quark pair is $s\bar{s}$ or $q\bar{q}$ ($q = d$ or u), based on the valence-quark composition of $\eta^{(\prime)}$.

The branching fractions are quite well measured for $B \rightarrow \eta'K$ and $B \rightarrow \eta K^*$. The mode $B^+ \rightarrow \eta K^+$ is established, but not yet the other charge state, $B^0 \rightarrow \eta K^0$. I present here preliminary results of an update of the search for the latter from *BABAR*, shown in Fig. 7 and Table I. This is based on the now complete $\Upsilon(4S)$ sample with 465 million $B\bar{B}$'s.

The neutral ηK decay is not yet clearly seen, though the two experiments combined give evidence for this mode with a branching fraction near 10^{-6} . There is some tension between this result and the value for the charged mode, as well as between *BABAR* and Belle for the charged mode.

I give a summary comparison between measurements and theoretical estimates for $\Delta S = 1$ P -

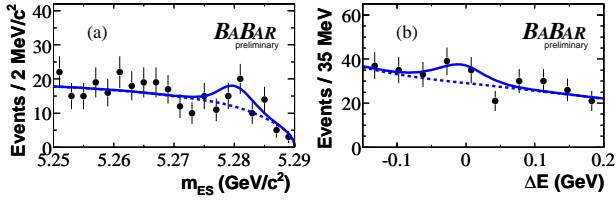


Figure 7: Projections of the *BABAR* data for $B^0 \rightarrow \eta K_S^0$ with fit function (solid curve) and background component (dashed curve) onto (a) the energy-substituted B mass, and (b) B -candidate energy residual.

Table I Measurements of branching fractions for $B \rightarrow \eta^{(\prime)} K$. The *BABAR* results for $B^0 \rightarrow \eta K^0$ are new here; the rest are from [20] (*BABAR*) and [21] (*Belle*).

Mode	<i>BABAR</i>	<i>Belle</i>	Average
ηK^0	$0.9_{-0.4}^{+0.5} \pm 0.1$ (< 1.6)	$1.1 \pm 0.4 \pm 0.1$ (< 1.9)	1.0 ± 0.3 (< 1.6)
ηK^+	$3.7 \pm 0.4 \pm 0.1$	$1.9 \pm 0.3_{-0.1}^{+0.2}$	2.7 ± 0.3
$\eta' K^0$	$66.6 \pm 2.6 \pm 2.8$	$58.9_{-3.5}^{+3.6} \pm 4.3$	64.9 ± 3.1
$\eta' K^+$	$70.0 \pm 1.5 \pm 2.8$	$69.2 \pm 2.2 \pm 3.7$	70.2 ± 2.5

P and $V-P$ decays (excluding those with combinations of pion and kaon) in Fig. 8. We see that the QCDF and SCET predictions accommodate the $\eta^{(\prime)} K^{(*)}$ branching fractions, but with large uncertainties. The biggest sources of uncertainty in these calculations are renormalization scale, quark masses, decay constants, form factors, and $\eta-\eta'$ mixing. The smaller errors in the $SU(3)$ fits reflect a greater dependence on the data themselves.

4.3. $\Delta S = 0$ $P-P$ and $V-P$ Decays

A group of flavor $SU(3)$ center states have been searched for by *BABAR*, with recent updates, including some preliminary results first presented here, based on 460 million $B\bar{B}$ pairs. Some of these branching-fraction limits contribute to relatively model-independent bounds on tree pollution in processes used to determine elements of the CKM matrix, such as $B^0 \rightarrow \eta' K^0$ and $B^0 \rightarrow \phi K^0$. Those are penguin-dominated decays for which only one weak phase is expected to appear, but this expectation depends on imperfectly understood strong interaction effects. The latter can be constrained from decays related by flavor $SU(3)$ [22], such as those shown in Table II.

In fact the latest limits don't improve much on the previous ones; instead they are showing evidence for some positive signals, e.g., for $B^0 \rightarrow \eta' \pi^0$ and $B^0 \rightarrow \eta^{(\prime)} \omega$.

A newly observed decay reported by *BABAR* based on the same sample [23] is $B^+ \rightarrow \eta \rho^+$; with a signal yield of 326_{-42}^{+44} events the branching fraction and

Table II Branching fractions with significance (S) and 90% C.L. upper limits, for B meson decays to $P-P$ and $V-P$ $SU(3)$ center states. The entries without citation are new preliminary results.

Mode	S (σ)	\mathcal{B} (10^{-6})	Ref.
$\eta\eta$	2.4	$0.8 \pm 0.4 \pm 0.1$ (< 1.4)	
$\eta'\eta$	1.4	$0.5 \pm 0.4 \pm 0.1$ (< 1.2)	[23]
$\eta'\eta'$	1.3	$0.9_{-0.7}^{+0.8} \pm 0.1$ (< 2.1)	
$\eta\pi^0$	2.2	$0.9 \pm 0.4 \pm 0.1$ (< 1.5)	[23]
$\eta'\pi^0$	3.1	$0.9 \pm 0.4 \pm 0.1$ (< 1.5)	[23]
$\eta\phi$	1.7	$0.22_{-0.15}^{+0.19} \pm 0.01$ (< 0.52)	
$\eta\omega$	3.5	$1.0_{-0.3}^{+0.4} \pm 0.1$ (< 1.6)	
$\eta'\phi$	1.3	$0.5 \pm 0.4 \pm 0.1$ (< 1.2)	
$\eta'\omega$	3.1	$1.0_{-0.4}^{+0.5} \pm 0.1$ (< 1.7)	
$\omega\pi^0$	0.3	$0.07 \pm 0.26 \pm 0.02$ (< 0.5)	[23]

charge asymmetry are found to be

$$\begin{aligned} \mathcal{B}(B^+ \rightarrow \eta \rho^+) &= (9.9 \pm 1.2 \pm 0.8) \times 10^{-6} \\ \mathcal{A}_{ch} &= 0.13 \pm 0.11 \pm 0.02. \end{aligned}$$

The branching fraction measured by *Belle* is considerably smaller: $\mathcal{B}(B^+ \rightarrow \eta \rho^+) = 4.1_{-1.3}^{+1.4} \pm 0.04$ [24].

A summary of the measurements and limits for $\Delta S = 0$ $P-P$ and $V-P$ B decays is given, along with theoretical estimates, in Fig. 9. As for the $\Delta S = 1$ decays, the trends are generally reproduced by the calculations, even though most theoretical errors are much larger than the experimental ones. The mode $B^0 \rightarrow \rho^\pm \pi^\mp$ seems to present the biggest challenge. Here the QCDF prediction has large uncertainties, coming from terms representing penguin annihilation and interactions with the spectator quark; SCET makes a prediction with smaller errors, resulting from greater use of experimental input, but giving a significantly lower branching fraction than is measured.

4.4. Decays to Axial Vector Mesons

In the last couple of years the study of charmless B meson decays has moved beyond the ground-state nonets to encompass some of the scalar, axial-vector, and tensor excitations. I present here some new and recent searches for states with a_1 and b_1 mesons.

In the quark model, the 1P_1 meson nonet contains $b_1(1235)$ with $I^G = 1^+$, two isosinglets $h_1(1380)$, $h_1(1170)$, and a strange isodoublet K_{1B} . The K_{1B} mixes with another state K_{1A} to form the physical $K_1(1270)$, $K_1(1400)$. The K_{1A} belongs to the 3P_1 meson nonet containing also the $a_1(1260)$ with $I^G = 1^-$, and isosinglets $f_1(1420)$, $f_1(1285)$. The decays $B^0 \rightarrow a_1(\pi, K)$ have been observed with the

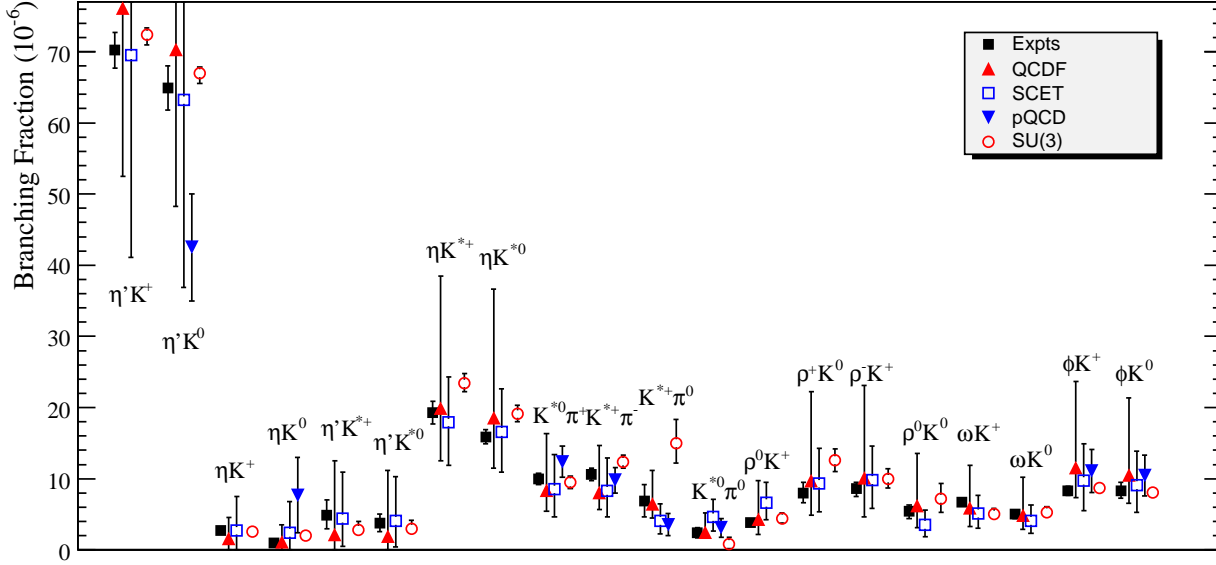


Figure 8: Measurements compared with theoretical estimates for $\Delta S = 1$ P - P and V - P decays.

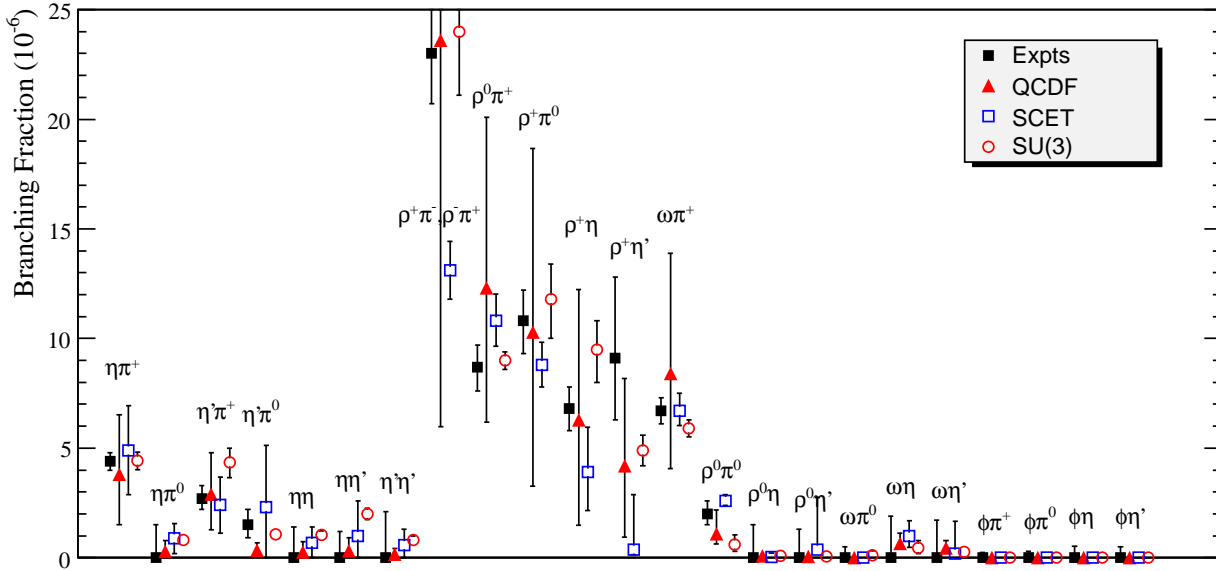


Figure 9: Measurements compared with theoretical estimates for $\Delta S = 0$ P - P and V - P decays.

following branching fractions:

$$\mathcal{B}(B^0 \rightarrow a_1^\mp \pi^\pm) = (33.2 \pm 3.8 \pm 3.0) \times 10^{-6} \quad [25]$$

$$= (29.8 \pm 3.2 \pm 4.6) \times 10^{-6} \quad [26]$$

$$\mathcal{B}(B^0 \rightarrow a_1^- K^+) = (8.2 \pm 1.5 \pm 1.2) \times 10^{-6} \quad [27]$$

$$\mathcal{B}(B^+ \rightarrow a_1^+ K^0) = (17.4 \pm 2.5 \pm 2.2) \times 10^{-6} \quad [27].$$

The significances of the recent observations of $B^0 \rightarrow a_1^- K^+$ and $B^+ \rightarrow a_1^+ K^0$ are 5.1 and 6.2 sigma, respectively.

The b_1 meson is observed through its dominant decay $b_1 \rightarrow \omega\pi$. CKM factors favor tree amplitudes for $b_1\pi$, and penguins for b_1K modes. The weak axial vector current is odd in G -parity, while b_1 is even, so the suppression of second-class weak currents implies a very small b_1 decay constant. Thus we expect that $\mathcal{B}(B^0 \rightarrow b_1^+ \pi^-) \ll \mathcal{B}(B^0 \rightarrow b_1^- \pi^+)$, and that $B^+ \rightarrow b_1^+ \pi^0$ is color-suppressed (as is $B^0 \rightarrow b_1^0 \pi^0$).

$BABAR$ reported observations of final states with b_1 accompanied by a charged kaon or pion last year [28]. Results of their new search for modes with b_1 and a

neutral kaon or pion [29] are given in Table III. The data show a clear signal for $B^+ \rightarrow b_1^+ K^0$, and evidence for $B^0 \rightarrow b_1^0 K^0$. Distributions of $B^+ \rightarrow b_1^+ K^0$ events that satisfy a requirement on the signal-to-total likelihood ratio that enhances the signal are shown in Fig. 10. For that mode the charge asymmetry is measured to be $-0.03 \pm 0.15 \pm 0.02$. Consistent with expectations, there is no sign of $B \rightarrow b_1 \pi^0$.

Table III Results of *BABAR*'s search for decays with b_1 and a neutral kaon or pion, based on 465 produced $B\bar{B}$'s. The columns give the signal yield Y_S , significance S , and branching fraction \mathcal{B} .

Mode	Y_S (ev.)	S (σ)	\mathcal{B} (10^{-6})
$b_1^+ K^0$	164^{+27}_{-25}	6.3	$9.6 \pm 1.7 \pm 0.9$
$b_1^0 K^0$	58^{+19}_{-17}	3.4	$5.1 \pm 1.8 \pm 0.5$
$b_1^+ \pi^0$	71^{+35}_{-32}	1.6	$1.8 \pm 0.9 \pm 0.2$
$b_1^0 \pi^0$	6^{+19}_{-16}	0.5	$0.4 \pm 0.8 \pm 0.2$

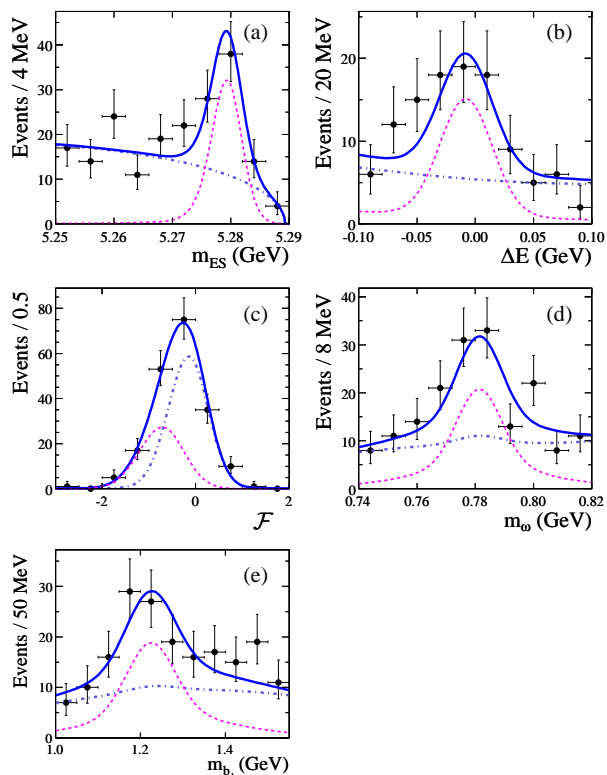


Figure 10: Projections of the *BABAR* data for $B^+ \rightarrow b_1^+ K^0$, with fit function (solid curve), signal component (dashed curve), and background component (dot-dashed curve), onto (a) the energy-substituted B mass, (b) ΔE , (c) event-shape Fisher discriminant, (d) ω mass, and (e) b_1 mass.

Theoretical estimates of the branching fractions of B mesons to $b_1 \pi$ and $b_1 K$ come from calculations based on naïve factorization [30], and on QCD factorization [31]. The latter incorporate light-cone dis-

tribution amplitudes evaluated from QCD sum rules, and predict branching fractions in quite good agreement with the measurements for these b_1 - P decays, as shown in Fig. 11. The naive-factorization calculations are rather sensitive to the mixing angle between K_{1A} and K_{1B} , for which data from other sources leave a two-fold ambiguity, but the comparison with these $B \rightarrow b_1$ decay measurements yields no consistent resolution of that ambiguity.

Cheng and Yang have extended their QCDF predictions to B decays involving pairs of vector and axial-vector mesons [32]. *BABAR* present here the preliminary result of a search for one of these, $B^0 \rightarrow b_1^\mp \rho^\pm$, for which the predicted branching fraction is a hefty 30×10^{-6} , about three times that of $B^0 \rightarrow b_1^- \pi^+$, due to the larger decay constant, $f_\rho > f_\pi$. The data, corresponding to 465 million $B\bar{B}$ pairs, are shown in Fig. 12. No signal is evident; the measured branching fraction is

$$\mathcal{B}(B^0 \rightarrow b_1^\mp \rho^\pm) = (-0.1 \pm 0.9 \pm 0.7) \times 10^{-6} \\ (< 1.7 \times 10^{-6}, 90\% \text{ C.L.}).$$

This result in disagreement with the theoretical estimate is somewhat surprising given the success of the predictions for the other measured b_1 modes.

5. Summary and Conclusions

I've selected several from an impressive array of new or very recent results in the decays of the B^+ and B_d mesons. The doubly Cabibbo-suppressed $B \rightarrow D_{(s)}(\pi, \rho)$ route to γ/ϕ_3 is still elusive, but progress is being made. Dibaryon systems from B meson decay show low-mass peaking, and suppression of 2-body modes; we are seeing new discoveries in baryon spectroscopy. Among decays to η and/or η' , there are many improved limits, observations of new decays and hints that more lie near the sensitivity horizon of experiments. Many new modes have been seen in decays to axial-vector states. Predictions are working quite well for A - P modes. Where are the A - V modes? Stay tuned. The global interplay between theory and experiment is expanding, and proving to be very productive.

Acknowledgments

I would like to thank my colleagues in the *BABAR* and Belle collaborations for their assistance in assembling the latest results for this review, and the organizers of the conference for their hospitality and skillfully organized program.

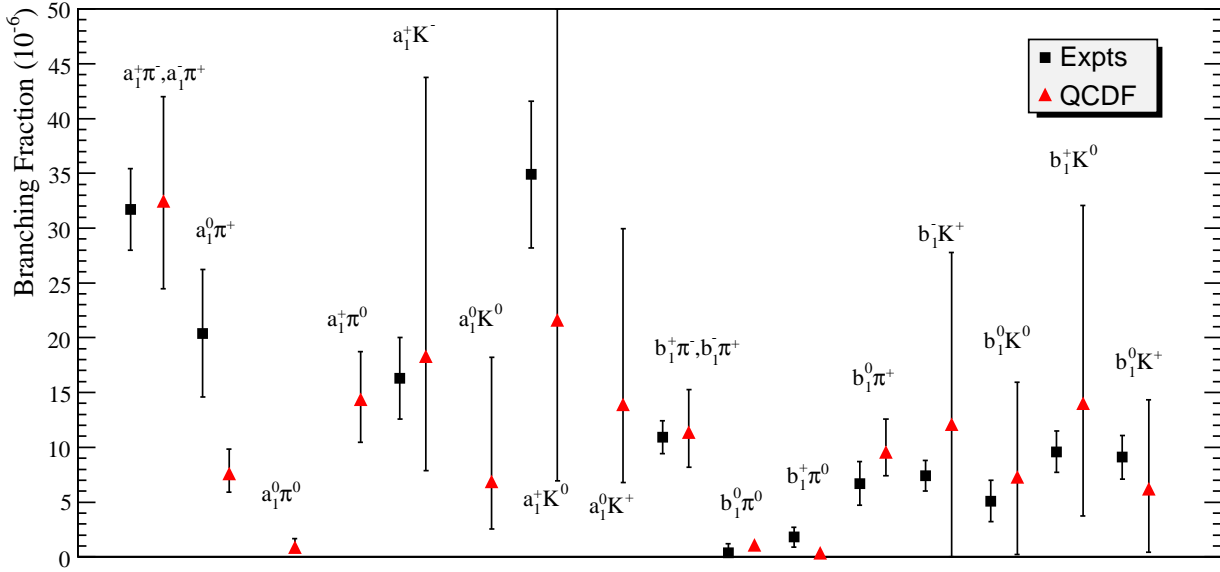


Figure 11: Measurements compared with theoretical estimates for $A-P$ decays.

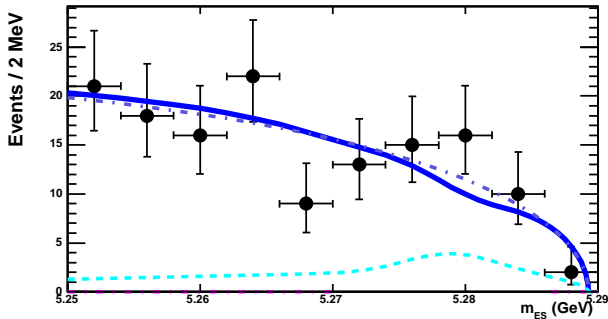


Figure 12: Signal-enhanced projection of the *BABAR* data for $B^0 \rightarrow b_1^\mp \rho^\pm$, with fit function (solid curve), peaking background component (dashed curve), and total background component (dot-dashed curve), onto the energy-substituted B mass.

References

- [1] Belle Collaboration, F. J. Ronga *et al.*, Phys. Rev. D **73**, 092003 (2006); *BABAR* Collaboration, B. Aubert *et al.*, Phys. Rev. D **73**, 111101 (2006).
- [2] Charge conjugate reactions are implicitly included here, and elsewhere in this paper unless otherwise indicated.
- [3] Belle Collaboration, M. Iwabuchi, M. Nakao *et al.*, Phys. Rev. Lett. **101**, 041601 (2008) [arXiv:0804.0831].
- [4] *BABAR* Collaboration, B. Aubert *et al.*, arXiv:0803.4296 [hep-ex] (2008).
- [5] Belle Collaboration, J. H. Chen, M. Z. Wang *et al.*, Phys. Rev. Lett. **100**, 251801 (2008).
- [6] *BABAR* Collaboration, B. Aubert *et al.*, arXiv:0807.4974 [hep-ex] (2008).
- [7] Belle Collaboration, R. Mizuk *et al.*, Phys. Rev. Lett. **94**, 122002 (2005).
- [8] Heavy Flavor Averaging Group, E. Barberio *et al.*, arXiv:0808.1297 (2008); <http://www.slac.stanford.edu/xorg/hfag>.
- [9] C-W. Chiang *et al.*, Phys. Rev. D **70**, 034020 (2004) [hep-ph/0404073]; J. Rosner, private communication.
- [10] C-W. Chiang *et al.*, Phys. Rev. D **69**, 034001 (2004) [hep-ph/0307395].
- [11] M. Bauer, B. Stech, and M. Wirbel, Z. Phys. C **34**, 103 (1987); G. Buchalla, A. Buras, and M. E. Lautenbacher, Rev. Mod. Phys. **68**, 1125 (1996).
- [12] A. Ali and C. Greub, Phys. Rev. D **57**, 2996 (1998); A. Ali, G. Kramer, and C. D. Lü, Phys. Rev. D **58**, 094009 (1998).
- [13] M. Beneke, G. Buchalla, M. Neubert, and C. T. Sachrajda, Phys. Rev. Lett. **83**, 1914 (1999) [hep-ph/9905312].
- [14] M. Beneke and M. Neubert, Nucl. Phys. B **675**, 333 (2003).
- [15] Alexander R. Williamson and Jure Zupan, Phys. Rev. D **74**, 014003 (2006); Wei Wang, Yu-Ming Wang, De-Shan Yang, Cai-Dian Lu, Phys. Rev. D **78**, 034011 (2008).
- [16] G. P. Lepage and S. Brodsky, Phys. Rev. D **22**, 2157 (1980); J. Botts and G. Sterman, Nucl. Phys. B **325**, 62 (1989); Y. Y. Keum *et al.*, Phys. Lett. B **504**, 6 (2001), Phys. Rev. D **63**, 054006 (2001); Y. Y. Keum and H. N. Li, Phys. Rev. D **63**, 074008 (2001).

- [17] Y.-Y. Keum., *Pramana* **63**, 1151-1170 (2004) [hep-ph/0410337].
- [18] E. Kou and A. I. Sanda, *Phys. Lett. B* **525**, 240 (2002).
- [19] M. Ciuchini *et al.*, *Nucl. Phys. B* **501**, 271 (1997) [hep-ph/9703353]; *Phys. Lett. B* **515**, 33 (2001) [hep-ph/0104126].
- [20] *BABAR* Collaboration, B. Aubert *et al.*, *Phys. Rev. D* **76**, 031103 (2007).
- [21] Belle Collaboration, P. Chang *et al.*, *Phys. Rev. D* **75** 071104 (2007); J. Schümann, C. H. Wang *et al.*, *Phys. Rev. Lett.* **97** 061802 (2006).
- [22] Yuval Grossman, Zoltan Ligeti, Yosef Nir, and Helen Quinn, *Phys. Rev. D* **68**, 015004 (2003); Michael Gronau, Jonathan L. Rosner, and Jure Zupan, *Phys. Rev. D* **74**, 093003 (2006).
- [23] *BABAR* Collaboration, B. Aubert *et al.*, *Phys. Rev. D* **78**, 011107 (2008).
- [24] Belle Collaboration, C. H. Wang *et al.*, *Phys. Rev. D* **75**, 092005 (2007).
- [25] *BABAR* Collaboration, B. Aubert *et al.*, *Phys. Rev. Lett.* **97**, 151802 (2006).
- [26] Belle Collaboration, K. Abe *et al.*, arXiv:0706.3279 [hep-ex] (2007).
- [27] *BABAR* Collaboration, B. Aubert *et al.*, *Phys. Rev. Lett.* **100**, 051803 (2008).
- [28] *BABAR* Collaboration, B. Aubert *et al.*, *Phys. Rev. Lett.* **99**, 241803 (2007).
- [29] *BABAR* Collaboration, B. Aubert *et al.*, *Phys. Rev. D* **78**, 011104 (2008).
- [30] V. Laporta, G. Nardulli, and T. N. Pham, *Phys. Rev. D* **74**, 054035 (2006); *Phys. Rev. D* **76**, 079903(E) (2007); G. Calderon, J. H. Munoz, C. E. Vera, *Phys. Rev. D* **76**, 094019 (2007).
- [31] H.-Y. Cheng and K.-C. Yang, *Phys. Rev. D* **76**, 114020 (2007).
- [32] H.-Y. Cheng and K.-C. Yang, arXiv:0805.0329 [hep-ph] (2008).